Comparison of ^{1}P–P Quenching with ^{1}P–CA Quenching and Acenaphthylene Photodimerization. Previously, with CA as quencher, we explained why A(cholesteric) >> A(isotropic) precludes mechanistic models which disregard cholesteric order. Crystal-packing considerations and CPK space-filling models indicate that in order for a P–CA exciplex-like quenching geometry to be attained in the cholesteric phase of CM, adjacent solvent layers must be disturbed. Furthermore, only if one of the components tilts out of the phase is effective overlap between the nitrogen lone-pair orbital and the π system of ^{1}P (the exciplex geometry[29]) achieved. Therefore, the solvent order decreases quenching efficiency by making the orientations appropriate for P–CA quenching less accessible. The overall effect is to increase the entropy of activation and energy of activation in the cholesteric phase.

In contrast, the quantum efficiency for the photodimerization of acenaphthylene is dramatically increased by the order of a cholesteric liquid-crystalline solvent.[30] Incorporation of the planar acenaphthylene in or between layers of the cholesteric phase and preferential plane-parallel diffusion of the solute results in an increased fraction of collisions which lead to products. Thus, cholesteric order facilitates the formation of the photodimer products.

The same diffusional motions and preferred collisional orientations apply to ^{1}P–P quenching and acenaphthylene dimerization when the reactions are conducted in cholesteric liquid-crystalline solvents. Diffusion parallel to the planes of the cholesteric layers results in collisional complexes from which quenching or product formation can proceed.

Dimerization of acenaphthylene is a relatively inefficient process in nonpolar, isotropic solvents, while the efficiency of ^{1}P–P quenching (i.e., quenching events per ^{1}P–P encounter) is near unity. Therefore, an increase in quenching efficiency in the cholesteric phase is not possible, and only if diffusion in the cholesteric phase of CM is less difficult than in its isotropic phase will E_3 be lowered. The increased viscosity of cholesteric CM relative to its isotropic phase makes this impossible.

A comparison of these three studies gives a general indication of the effects which can be expected when bimolecular reactions are conducted in cholesteric liquid-crystalline media. If the isotropic reaction probability per encounter is less than unity, the ordering of solutes imposed by the cholesteric phase may result in an increase or decrease in reaction efficiency. If the phase orients the reactants such that collisions leading to product are more probable (as in the acenaphthylene case), reaction probability will be increased. If, on the other hand, the cholesteric phase makes the preferred collisions less probable (as in the ^{1}P–CA case), the efficiency of the reaction is decreased. Finally, if the reaction probability per encounter in the isotropic phase is near unity, the presence of solvent order can result in a decreased or unchanged (as in the ^{1}P–P case) reaction efficiency.

Conclusions

Employing methods developed recently, analyses of dynamic and steady-state fluorescence data indicate that the relative orientations for ^{1}P quenching by P and excimer formation are similar in the cholesteric and isotropic phases of CM. That E_3(cholesteric) is only slightly greater than E_3(isotropic) and A_3(cholesteric) is slightly larger than A_3(isotropic) suggest that decreased ^{1}P quenching efficiency in the cholesteric phase is a result of increased viscosity. Space-filling models (CPK) and crystal-packing considerations indicate that formation of an excimer-like transition state for quenching, in which the molecules are oriented parallel to one another and to the planes of the cholesteric phase, does *not* significantly disrupt solvent order. Comparison of these data and those for ^{1}P quenching by CA and photodimerization of acenaphthylene demonstrate that a cholesteric liquid-crystalline medium can be used to differentiate various quenching transition-state geometries on the basis of their shapes. Investigations in which exciplex formation is expected to be much more dependent upon the viscosity of a cholesteric phase than its order (as in the ^{1}P–P excimer studied here) are in progress.

Acknowledgment. The National Science Foundation (Grant CHE-7906572) and the Naval Research Laboratory are acknowledged for financial support of this research.

Registry No. Pyrene, 129-00-0.

(29) (a) Meeus, F.; Van der Auweraer, M.; Dederen, J. C.; DeSchryver, F. C. *Recl. Trav. Chim. Pays-Bas* **1979**, *98*, 220. (b) Taylor, G. N.; Chandross, E. A.; Schiebel, A. H. *J. Am. Chem. Soc.* **1974**, *96*, 2693.

(30) Nerbonne, J. M.; Weiss, R. G. *J. Am. Chem. Soc.* **1979**, *101*, 409.

Dynamics of Interfacial Electron-Transfer Processes in Colloidal Semiconductor Systems

Dung Duonghong, Jeremy Ramsden, and Michael Grätzel*

Contribution from the Institut de Chimie Physique, Ecole Polytechnique Fédérale, CH-1015 Lausanne, Switzerland. *Received July 29, 1981*

Abstract: The dynamics of interfacial electron-transfer reactions were studied with colloidal TiO_2 and CdS particles, which form transparent aqueous dispersions. Excitation of the semiconductor was carried out by a nanosecond laser flash and subsequent conduction-band electron (e^-_{CB}) and hole (h^+) transfer reactions to solution species examined by kinetic spectroscopy. Methylviologen (MV^{2+}) was employed as an electron acceptor and thiocyanate or a phenothiazine derivative as a hole scavenger. Excitation of colloidal TiO_2 leads to long-lived e^-_{CB} whose rate of reaction with MV^{2+} is strongly influenced by the MV^{2+} concentration and pH. The pH effect on the yield of MV^+ can be exploited to derive the flat-band potential of the particle for which a value of E_{fb} = 0.130 − 0.059(pH) V (vs. NHE) was obtained. In the case of colloidal CdS the lifetime of the electron-hole pair was determined as 0.3 ns from time-resolved fluorescence spectroscopy. Only donors or acceptors adsorbed onto the particle surface can intervene as h^+ or e^-_{CB} scavengers, respectively. Experiments with Pt-loaded CdS established the competition of catalytic H_2 production by e^-_{CB} with electron transfer to adsorbed MV^{2+}. RuO_2 deposits are shown to enhance hole transfer from the valence band to solution species.

Interfacial electron-transfer processes play a crucial role in light-energy conversion devices where semiconductor–electrolyte junctions are employed as light-harvesting units. In view of the importance of these devices for the utilization of solar energy, it is highly desirable to obtain detailed experimental information on the dynamics of photoinduced conduction or valence-band processes involving species in solution. In the case of solid semiconductor electrodes, a direct study of the kinetics of these re-

0002-7863/82/1504-2977$01.25/0

actions is made exceedingly difficult[1] by the response of the electrical circuit to phenomena unrelated to the electron-transfer event at the interface. Similarly, the study of macrodispersions of semiconductor powders is hampered by the high turbidity of these systems, rendering impossible the observation of transient species by fast kinetic spectroscopy.

In connection with our present program on the light-induced cleavage of water into hydrogen and oxygen,[2] we became intrigued with the idea of investigating monodisperse semiconducting particles of small enough dimensions to render scattering of light negligible. These have the advantage of yielding optically transparent dispersions, allowing for ready kinetic analysis of interfacial charge-transfer processes by laser photolysis techniques.[3] In a previous investigation, we examined the kinetics of electron injection into colloidal TiO_2 particles following light-induced charge transfer from an excited sensitizer to an electron relay in solution.[4] In the present report, the colloidal semiconductor particles are directly excited by band-gap irradiation. The subsequent reaction of conduction-band electrons and valence-band holes with reactants in solution is followed by using laser photolysis techniques. The competitive trapping of electrons by noble-metal catalysts, deposited onto the semiconductor particle to mediate hydrogen generation from water, is investigated. Finally, this study establishes a technique to determine the flat-band potential of ultrafine colloidal semiconductors.

Experimental Section

Materials. Titanium tetraisopropoxide (Ventron GMBH), methylviologen (BDH), and H_2PtCl_6 (Engelhard) were used as supplied. Deionized water was refluxed over alkaline permanganate and subsequently distilled twice from a quartz still. All other reagents were at least analytical grade and were used as supplied.

Preparation of Colloidal Semiconductors. Colloidal particles of TiO_2 were prepared through hydrolysis of titanium tetraisopropoxide in acidic (HCl, pH 1.5) aqueous solution.[4] A transparent TiO_2 sol is thus obtained containing 500 mg/L TiO_2, which is stable at pH ≤ 3. X-ray diffraction analysis revealed that the particles are mainly amorphous with a small percentage of anatase. Their hydrodynamic radius is 200 Å and the polydispersity is surprisingly low as determined from quasi-elastic light-scattering measurements. The TiO_2 sol does not absorb in the visible spectrum; a sharp absorption band rises toward the UV spectrum at $\lambda \leq 380$ nm. The onset of this absorption corresponds to a band gap of approximately 3.2 eV. From electrophoretic measurements, the point of zero ζ potential (PZZP) is derived as 3.3.[4]

For investigations above pH 3, it was necessary to employ a stabilizing agent for the TiO_2 sol. Poly(vinyl alcohol) (0.1% solution, M_r = 60 000) was employed. It was added to the acidic solution of the sol, and the pH was subsequently raised by removing the HCl via a 30-min treatment with Amberlite MB3 exchange resin. Final adjustment of the pH was carried out by adding HCl or NaOH.

For the preparation of colloidal CdS solutions, 5×10^{-4} mol of $Cd(NO_3)_2$ was dissolved in 100 mL of a neutral aqueous 10^{-2} M solution of sodium hexametaphosphate. The mixture was transferred into a flask and H_2S passed above the solution until the yellow color of the CdS sol had fully developed and no further absorbance changes could be detected (the time required for completion of this process is ca. 1 min). For removal of excess H_2S, the solution was subsequently flushed with argon for at least 30 min. The final pH of the dispersion was around 3 and was adjusted to the experimentally desired value by addition of HCl or NaOH.

The onset of the absorption of the CdS particles was found to be located at 520 nm, which coincides with the 2.4-eV band gap of CdS. The band rises toward the UV spectrum in a very steep fashion, which is typical for electronic transitions in direct band-gap semiconductors.[5]

Two methods were employed to assess the size of the colloidal CdS particles. Transmission electron microscopy, performed with a Phillps EM300 instrument, showed the presence of approximately spherical particles with a mean radius of 40 Å. Dark-field micrographs revealed that most of the particles consisted of single crystals. The lattice constants obtained from the electron-diffraction pattern indicate the presence of a wurtzite structure. The size of the particles was also determined by quasi-elastic light-scattering technique. Correlation functions obtained were strictly exponential over several lifetimes, indicating very low polydispersity. The hydrodynamic radius derived from these functions is 60 Å, which is in satisfactory agreement with the electron-microscopy results.

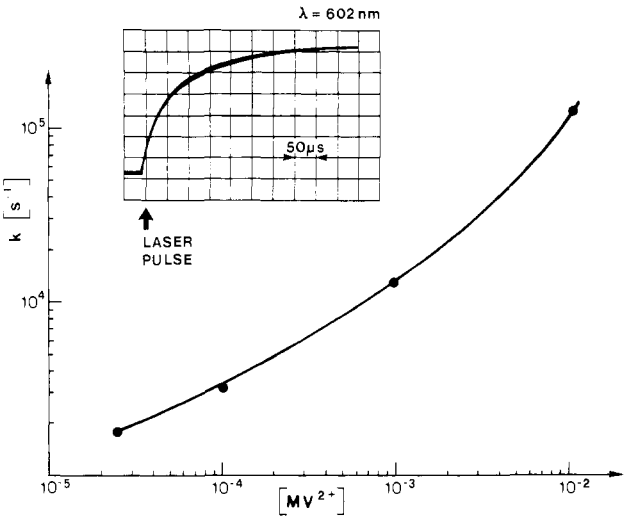

Figure 1. 347.1-nm laser photolysis of colloidal TiO_2 (500 mg/L, pH 5). The observed rate constant for MV^+ formation is plotted against MV^{2+} concentration. Insert: oscilloscope trace illustrating time course of 602 absorbance for $[MV^{2+}] = 10^{-3}$ M.

For loading the CdS particles with Pt, H_2PtCl_6 (0.4–3 mg) was added together with a 40% aqueous solution of formaldehyde to 25 mL of CdS sol containing 110 mg of CdS/L. After deoxygenation Pt was deposited onto the CdS particles via photoplatinization.[6,7] The excess of formaldehyde was subsequently removed under vacuum.

Apparatus. Laser-photolysis experiments were performed with a JK-2000 frequency-doubled (347 nm) ruby laser with a pulse width of 15 μs. For excitation of the CdS particles, a JK-2000 frequency-tripled (353 nm) neodymium laser or a Phase-R, Model DL-2100C flash light pumped dye laser (dye Green 2, λ = 482 nm) was employed. The photomultiplier system used for kinetic spectroscopy has already been described.[8] The time course of the optical events was recorded either with a fast rise time oscilloscope or with a Tektronix-WP 2221 data acquisition system equipped with two R-7912 transient digitizers. Fluorescence spectra were run on a Hitachi Perkin-Elmer MPF-44A spectrofluorimeter. Emission lifetimes were obtained with a PRA single photon counting instrument. Quasi-elastic light-scattering experiments were performed with a Krypton ion laser (Coherent, Model 3000) as a light source. Scattering experiments using wavelengths of 520.9, 530.9, 568, and 647 nm gave consistent results. An EMI 9663 photomultiplier in conjunction with the photon counter and a Langley-Ford correlator were employed for detection and analysis of the data.

Results and Discussion

Dynamics of Electron Transfer from the Conduction Band of Colloidal TiO_2 to Acceptors in Solution. Flat-Band Potential of Colloidal TiO_2 Particles. In order to study the dynamics of electron transfer from colloidal TiO_2 particles across the interface to solution species, we chose methylviologen (MV^{2+}) as an electron acceptor. This has the advantage of undergoing a reversible one-electron reduction with a well-defined and pH-independent redox potential (E° = −440 mV against NHE). Furthermore, the reduced form (MV^+) can be readily identified by its characteristic blue color corresponding to an absorption maximum of 602 nm (ϵ 11 000 M^{-1} cm^{-1}).[9]

(1) Deutscher, S. B.; Richardson, J. H.; Perone, S. P.; Rosenthal, J.; Ziemer, J. *Faraday Discuss. Chem. Soc.* **1980**, *70*, 2.
(2) Grätzel, M. *Ber. Bunsenges. Phys. Chem.* **1980**, *84*, 481. Borgarello, E.; Kiwi, J.; Pelizzetti, E.; Visca, M.; Grätzel, M. *Nature (London)* **1981**, *284*, 158; *J. Am. Chem. Soc.* **1981**, *103*, 6324 and references cited therein.
(3) Grätzel, M. *Acc. Chem. Res.* **1981**, *14*, 376.
(4) Duonghong, D.; Borgarello, E.; Grätzel, M. *J. Am. Chem. Soc.* **1981**, *103*, 4685.
(5) Butler, M. A. *J. Appl. Phys.* **1977**, *48*, 1914.
(6) Kalyanasundaram, K.; Borgarello, E.; Grätzel, M. *Helv. Chim. Acta* **1981**, *64*, 362.
(7) Kraeutler, E.; Bard, A. J. *J. Am. Chem. Soc.* **1978**, *100*, 4318.
(8) Rothenberger, G.; Infelta, P. P.; Grätzel, M. *J. Phys. Chem.* **1979**, *83*, 1871.
(9) Trudinger, P. A. *Anal. Biochem.* **1970**, *36*, 222.

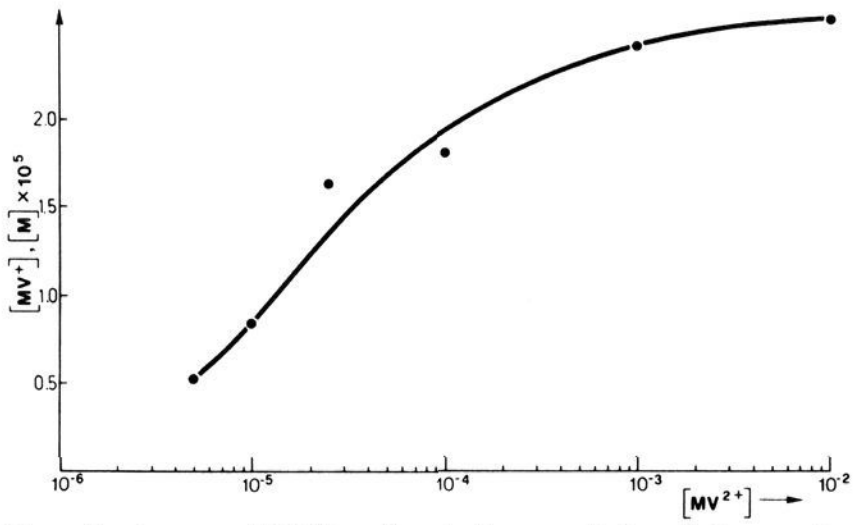

Figure 2. Amount of MV^+ produced after completion of e^-_{CB} reaction with MV^{2+}; conditions as in Figure 1.

Upon exposure of a deaerated TiO_2 sol to near-UV light in the presence of MV^{2+}, the formation of this blue species becomes readily apparent. Figure 1 shows data obtained from the 347-nm laser photolysis of solutions containing colloidal TiO_2 (500 mg/L, pH 5) and different concentrations of MV^{2+}. Inserted is an oscilloscope trace illustrating the time course of the 602-nm absorbance for $[MV^{2+}] = 10^{-3}$ M. A pronounced growth departing from the base line after laser excitation of TiO_2 is observed that attains a plateau after ca. 500 μs. Thereafter, no further changes are noted over a time scale of at least several hundred milliseconds. Blank experiments established that generation of MV^+ results from band-gap excitation of the colloidal TiO_2 particles. Thus, only a negligible amount of MV^+ ($\sim 10^{-7}$ M) is produced if a solution containing 10^{-2} M MV^{2+}, i.e., the maximum concentration employed in this study, is subjected to 347-nm laser photolysis.

Kinetic evaluation of the oscillograms showed that the growth of the 602-nm absorption follows a first-order rate law under conditions[10] where $[MV^{2+}] \geq 10^{-4}$ M. The observed rate constant k increases linearly with MV^{2+} concentration, indicating pseudo-first-order behavior. Figure 1 shows a logarithmic presentation of the data. This was chosen to facilitate inspection of the results, which cover a wide concentration range. A plot of k against MV^{2+} concentration for $[MV^{2+}] \geq 2.5 \times 10^{-5}$ M yields a straight line with a slope of 1.2×10^7 M^{-1} s^{-1}, which corresponds to the second-order rate constant for reduction of MV^{2+} by excited TiO_2 particles.

The amount of MV^+ produced after completion of the growth process depends on the initial MV^{2+} concentration present in the solution (Figure 2). At relatively low acceptor concentration ($[MV^{2+}] \leq 2 \times 10^{-5}$ M), the concentration of reduced viologen is practically equal to that of MV^{2+}, $[MV^+]_{t\to\infty} = [MV^{2+}]_{t=0}$, indicating that the latter is quantitatively reduced. The curve levels off at higher MV^{2+} concentration where it approaches a limit of $(MV^+) = 3.5 \times 10^{-5}$ M.

These observations may be interpreted in terms of band-gap excitation of the colloidal TiO_2 particles resulting in electron-hole pair production (Figure 4). The electron is subsequently transferred from the conduction band to the MV^{2+} acceptor in solution, the growth of the MV^+ absorption reflecting the kinetics of this interfacial charge-transfer reaction. This process does not appear to involve MV^{2+} species absorbed to the surface of TiO_2, since in such a case prompt appearance of MV^+ concomitantly and within the laser pulse would be expected. The rather gradual formation of MV^+, which takes place in the micro-to-millisecond time domain after laser excitation, would indicate that the conduction-band electrons (e^-_{CB}) react with MV^{2+} present in the solution bulk and diffusing toward the TiO_2 surface. Such a model is further supported by the finding that the reaction rate increases linearly with MV^{2+} concentration. If the latter were adsorbed to the TiO_2 particles, the rate of electron transfer would be expected to level off at higher MV^{2+} concentration where saturation of available surface sites is reached.

(10) At lower MV^{2+} concentration the concentration of conduction-band electrons produced by the laser is equal to or even higher than that of methylviologen. The reciprocal first half-life time was used to calculate the rate constant for electron transfer.

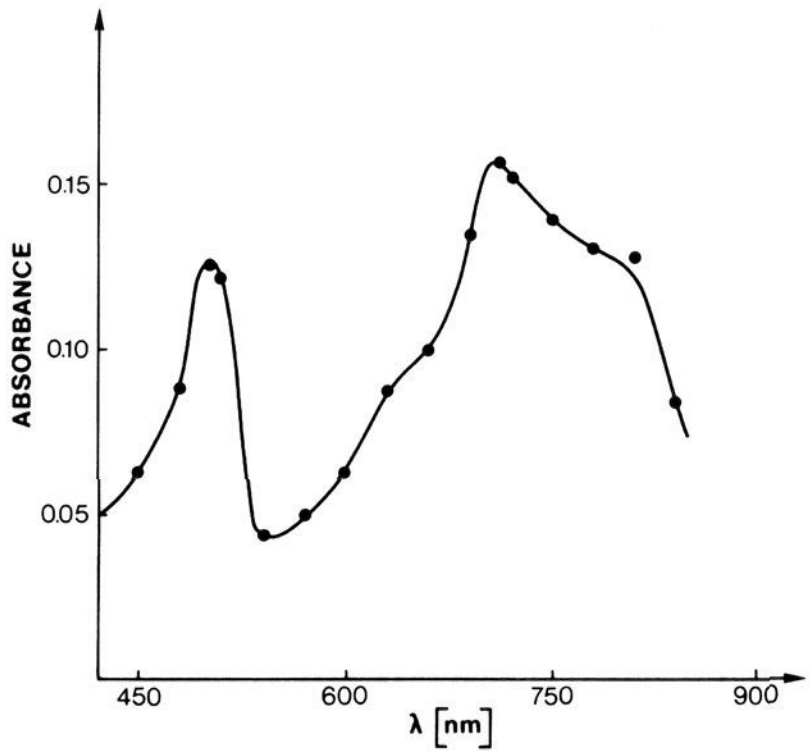

Figure 3. Absorption spectrum of a colloidal TiO_2 dispersion irradiated for 30 min with the >300 nm output of a 450-W Xe lamp. An unirradiated TiO_2 dispersion was placed in the reference light beam. Analytical TiO_2 concentration = 2 g/L. The sample was deaerated prior to illumination.

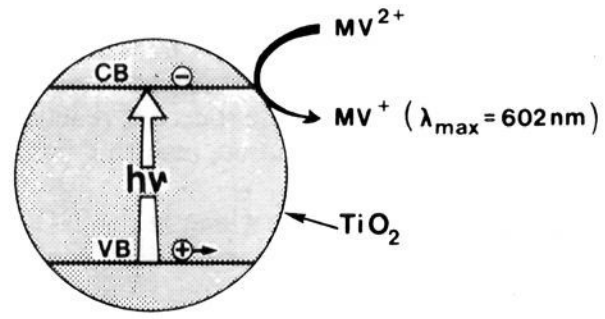

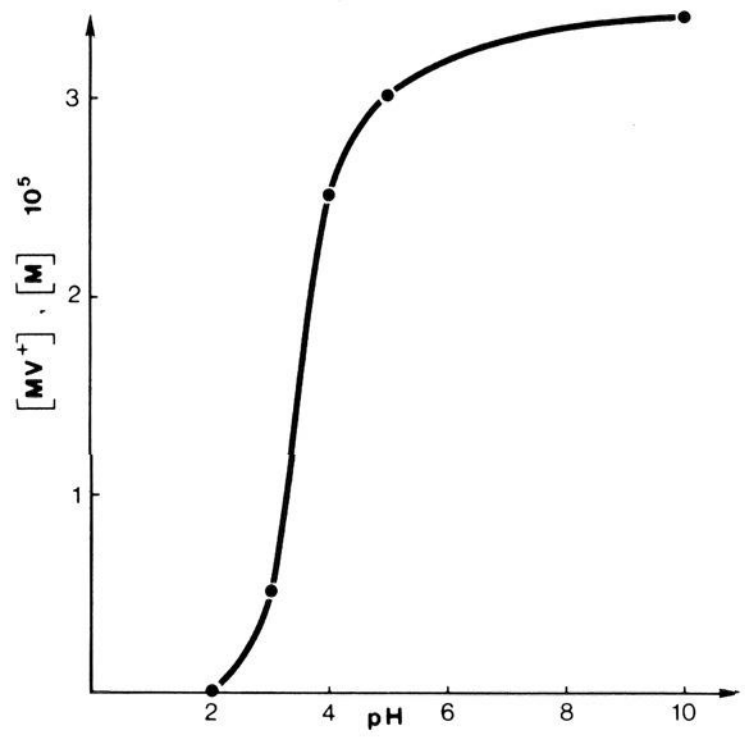

Figure 4. Effect of pH on the yield of MV^+ after completion of interfacial electron-transfer colloidal TiO_2 (500 mg/L); $[MV^{2+}] = 10^{-3}$ M.

It should be noted that the rates reported in Figure 7 are lower than those predicted for a diffusion-controlled reaction. If one inserts in Smoluchowski's equation ($k_{tr} = 4\pi N_A Dr/1000$) an effective reaction radius of 200 Å and the diffusion coefficient of MV^{2+} (9×10^{-6} cm^2 s^{-1}), one calculates $k_{tr} \simeq 1.3 \times 10^{11}$ M^{-1} s^{-1}. The measured value for the bimolecular rate constant for the reduction of MV^{2+} by TiO_2 conduction-band electrons is, however, only 1.2×10^7 M^{-1} s^{-1}. One concludes that at pH 5 interfacial electron transfer does not take place upon every encounter between TiO_2 particles and MV^{2+}. As for the complementary reaction

of the valence-band hole, it comprises, under the conditions applied in Figure 1, oxidation of water to oxygen and/or oxidation of the protective agent poly(vinyl alcohol). At lower pH values, where no stabilizing polymer was employed, water oxidation is the only pathway of reaction. These hole-transfer processes will be discussed further below.

The explanation of the effect of MV^{2+} on the yield of MV^+ (Figure 2) is based on the concentration of electron-hole pairs ($e^-_{CB} \cdots h^+$] produced by the laser pulse. At low MV^{2+} concentration [$e^-_{CB} \cdots h^+$] $\gg$ [MV^{2+}], and therefore the latter is quantitatively reduced. The inverse condition hold at high MV^{2+} concentration where [$e^-_{CB} \cdots h^+$] $\ll$ [MV^{2+}]. The reduction of MV^{2+} is incomplete in the latter case and reaches a limit when [e^-_{CB}] = [MV^+]. This allows us to derive the electron-hole pair concentration produced by the light flash, which according to Figure 2 is around 2.6×10^{-5} M. By dividing this number through the concentration of photons adsorbed by the solution,[11] one calculates a quantum efficiency of practically 100% for the production of MV^+. This shows that all the conduction-band electrons can be scavenged by acceptor ions at fairly low concentration of the latter.[12]

A final point to be discussed in connection with Figures 1 and 2 concerns the lifetime of conduction-band electrons in the TiO_2 particle. At the lowest concentration of MV^{2+} employed, the growth of MV^+ occurs over a period of at least several milliseconds, implying that e^-_{CB} lives at least over the same time span. From this finding one could be led to infer that the lifetime of an $e^- \cdots h^+$ pair in a colloidal TiO_2 particle is at least several milliseconds. However, such a reasoning neglects the possibility that the hole could be rapidly removed from the sphere of reaction by trapping in a surface state or water oxidation, resulting in a long survival time of e^-_{CB}.

That the lifetime of e^-_{CB} is very long in the TiO_2 particles was independently shown in continuous irradiation experiments. A concentrated transparent TiO_2 sol (2 g/L) was prepared by hydrolysis of titanium tetraisopropoxide in 1 M HCl. Subsequently, the sol was subjected to dialysis over a period of 10 h until the solution pH had increased to 3. The 2-propanol was quantitatively removed under vacuum. After deoxygenation the TiO_2 sol was irradiated with near-UV light. A blue color appeared after ca. 30 min of exposure. The spectrum of such an irradiated dispersion is shown in Figure 3. It exhibits a broad featureless absorption in the wavelength domain between 550 and 900 nm with a maximum around 900 nm. A second sharper and somewhat weaker band appears with a maximum around 500 nm. One might be tempted to attribute the latter absorption to the $t_{2g} \rightarrow e_g$ transition of the $Ti(H_2O)_6^{3+}$ ion, which is indeed centered around 500 nm. However, as the extinction coefficient associated with this transition is very small, 5 M^{-1} cm^{-1}, an absorbance of 0.12 could not be obtained even if 50% of all the TiO_2 (2.6×10^{-2} M) were converted into $Ti(H_2O)_3^{3+}$. Presumably, the 500-nm peak arises from Ti^{3+} ions located in the surface region of the particles. The broad bend in the red, on the other hand, is ascribed to optical excitation of conduction-band electrons. Interestingly, when the irradiation is stopped, the color disappears and hydrogen is evolved concomitantly. Hydrogen generation is also observed in the photostationary state where it proceeds at a rate of 200 μL/h (solution volume 25 mL, 450-W Xe lamp). These results stand in close relation to the observation of Bard et al.,[13] who discovered a shift in the isoelectric point if TiO_2 powder suspensions were illuminated by band-gap irradiation. This was attributed to the accumulation of electrons in the conduction band of the TiO_2 particles. A cell device was constructed that allowed the collection of the electrons from such a TiO_2 slurry at an electrode as anodic photocurrent. We observe similar effects with our TiO_2 sol: if a Pt electrode polarized to +400 mV (NHE) is dipped into the colloidal TiO_2 dispersion (0.01 M HCl) irradiated with a 1000-W Xe lamp, an anodic photocurrent of ca. 20 $\mu A/cm^2$ is produced, resulting from the discharge of illuminated TiO_2 particles.[14] These findings strongly corroborate the laser photolysis results, from which a surprisingly long lifetime of the conduction-band electron in the colloidal TiO_2 particle was inferred. Valence band holes produced during photolysis generate oxygen from water. This consumes part of e^-_{CB} under formation of O_2^- which is chemisorbed onto the TiO_2 sol.

The band position of TiO_2 is known to be shifted by 59 mV upon changing the pH by one unit.[15] This is expected to affect the efficiency and rate of an interfacial electron-transfer process with a couple such as MV^{2+}/MV^+ whose redox potential is pH independent. In Figure 4 is illustrated the effect of pH on the yield of MV^+ after completion of the electron transfer. (In these experiments the MV^{2+} concentration was maintained at 10^{-3} M.) This curve exhibits a sigmoidal shape; no reduction of MV^{2+} occurs at pH $\leq$2. The yield of MV^+ increases steeply between pH 2.5 and 5 and attains a plateau for neutral and basic solutions where [MV^+] = 3.5×10^{-5} M.

The results depicted in Figure 4 can be used to derive the flat-band potential (E_{fb}) of the colloidal TiO_2 particles. The reasoning is as follows: Due to an intrinsic oxygen deficiency, TiO_2 is an *n*-type semiconductor with the Fermi level (E_f) more or less close to the conduction band (E_{CB}). Laser excitation of TiO_2 leads to nonequilibrium population in e^-_{CB} and h^+ and therefore splitting of E_f into two quasi-Fermi levels, one for the hole and one for the electron, $E_f(e^-)$. The latter practically merges with the conduction band as the carrier density produced by the laser flash in the TiO_2 particles[16] exceeds 10^{19} cm^{-3}. In the presence of MV^{2+}, $E_f(e^-)$ will equilibrate with the Fermi level of the redox couple in solution

$$E_f(e^-) = E_f(MV^{2+}/MV^+) \quad (1)$$

or

$$E_f(e^-, \text{pH } 0) - 0.059(\text{pH}) = E^\circ(MV^{2+}/MV^+) + 0.059 \log ([MV^{2+}]/[MV^+]) \quad (2)$$

where $E^\circ(MV^{2+}/MV^+) = -0.445$ V (vs. NHE).[17] The equilibrium

$$e^-_{CB} + MV^{2+} \rightleftharpoons MV^+ \quad (3)$$

is established once the electron-transfer process has come to completion, i.e., in the plateau region of the MV^+ growth curve such as is depicted in Figures 1 and 6. At low pH values this equilibrium is displaced to the left due to the anodic shift of the position of the TiO_2 conduction band with increasing proton concentration. Under these conditions, only a small fraction of the conduction-band electrons produced by laser excitation will leave the TiO_2 particle and form MV^+. As the overwhelming part of electrons stay within the colloidal semiconductor, the condition

$$E_f(e^-) \simeq E_{CB}(TiO_2) \simeq E_{fb}(TiO_2) \quad (4)$$

remains valid after equilibration has taken place.[18] Under

(11) Calculated from the optical density of the solution at 347 nm and the incident laser photon flux. Uncertainty in the irradiated volume introduces an ca. 25% error in this determination.

(12) Honda et al. (paper submitted to *J. Phys. Chem.*) have determined a quantum yield of 1 for MV^{2+} reduction in illuminated TiO_2 powder suspensions. This is in excellent agreement with our results obtained from colloidal dispersions. We thank Professor Honda for informing us of his results prior to publication.

(13) (a) Dunn, W. W.; Aikawa, Y.; Bard, A. J. *J. Am. Chem. Soc.* **1981**, *103*, 3456. (b) Dunn, W. W.; Aikawa, Y.; Bard, A. J. *J. Electrochem. Soc.* **1981**, *128*, 222.

(14) Geiger, T., unpublished results.

(15) The flat-band potential of a TiO_2 electrode shifts cathodically with increasing pH: at T = 25 °C, the relation is $E_{fb} = E_{fb}$ (pH 0) - 0.059(pH).

(16) The concentration of TiO_2 particles calculated from their hydrodynamic radius (R_H = 200 Å) and the bulk density of TiO_2 is 1.2×10^{-8} M. Since the concentration of electron-hole pairs produced is about 3×10^{-5} M, one calculates the number of electrons per particles as ca. 3000. Taking into account that a sphere of radius R = 200 Å has a volume of 3.4×10^{-17} cm^3, the carrier density is about 10^{20} cm^{-3}.

(17) Michaelis, L.; Hill, E. S. *J. Gen. Physiol.* **1933**, *16*, 859.

(18) In view of the minute size of the TiO_2 particle as well as the fact that only a minor fraction of e^-_{CB} produced by the laser pulse leaves the particle to reduce MV^{2+}, one can neglect the formation of a depletion layer and hence band bending at low pH. At high pH, practically all of the electrons leave the TiO_2 particle. $E_f(e^-)$ is here significantly below the conduction band after completion of the electron transfer to MV^{2+}, and band bending can no longer be neglected.

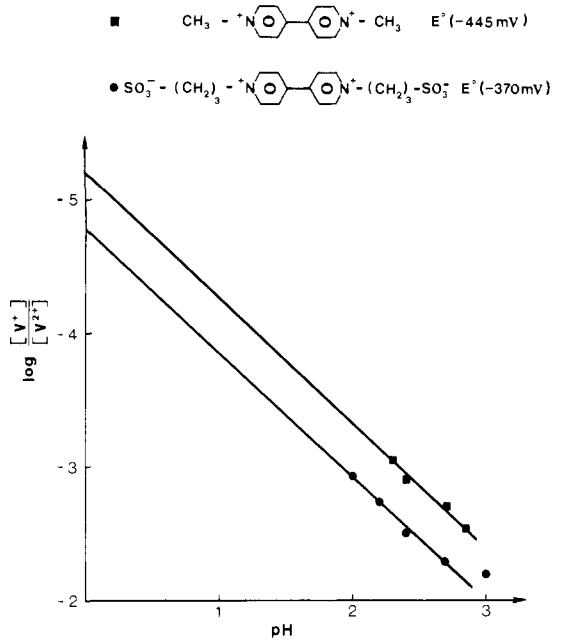

Figure 5. Laser-photolytic determination of the flat-band potential of colloidal TiO_2 particles. Two different viologens, i.e., MV^{2+} (E° = −0.445 V) and PVS (E° = −0.370 V), are employed as electron acceptors (viologen concentration = 10^{-3} M). The ratio V^+/V^{2+}, measured after completion of electron transfer, is plotted in a semilogarithmic fashion as a function of pH.

equilibrium the ratio of reduced to nonreduced viologen should be given by

$$\log \frac{[MV^+]}{[MV^{2+}]} = \frac{E^\circ(MV^{2+}/MV^+) - E_{fb}(TiO_2, \text{pH } 0)}{0.059} - \text{pH} \tag{5}$$

where $E_{fb}(TiO_2, \text{pH } 0)$ is the flat-band potential of a colloidal TiO_2 particle at pH 0.

The validity of relation 5 was tested by careful determination of the MV^+/MV^{2+} ratio at different H^+ concentrations below pH 3. The concentration of MV^+ was always measured after completion of the electron-transfer process (eq 3), and no protective agent was employed to stabilize the TiO_2 particles. A plot of the data according to eq 5 is shown in Figure 5. A straight line with a slope of −1 is obtained in agreement with the prediction of this equation. From the extrapolated intercept, one obtains for the flat-band potential of the colloidal TiO_2 particle

$$E_{fb}(TiO_2, \text{pH } 0) = -0.14 \text{ V (vs. NHE)}$$

An independent confirmation of this result was obtained from experiments where the zwitterionic propylviologen sulfonate (PVS^0) was used as an electron acceptor. The redox potential of the PVS^0/PVS^- couple is 75 mV more positive than that of MV^{2+}. Data obtained with this system are included in Figure 5. A straight line with a slope of 1 is again obtained, which for a given pH is displaced to higher concentration of reduced viologen, as expected from eq 5. The intercept with the ordinate corresponds to $E_{fb}(TiO_2, \text{pH } 0)$ = −0.1 V (vs. NHE), which in view of the experimental errors in determining the small concentrations of reduced viologen, as well as the large extrapolation made in Figure 5, is in remarkably good agreement with the value derived from the experiments with MV^{2+}. The flat-band potential for our colloidal TiO_2 particles is therefore evaluated as

$$E_{fb}(TiO_2) = -(0.12 \pm 0.02) - 0.059(\text{pH}) \text{ V (vs. NHE)}$$

for a temperature of 25 °C.

It is instructive to compare this value with the flat-band potential determined for single-crystal rutile electrodes. Gomes et al.[19]

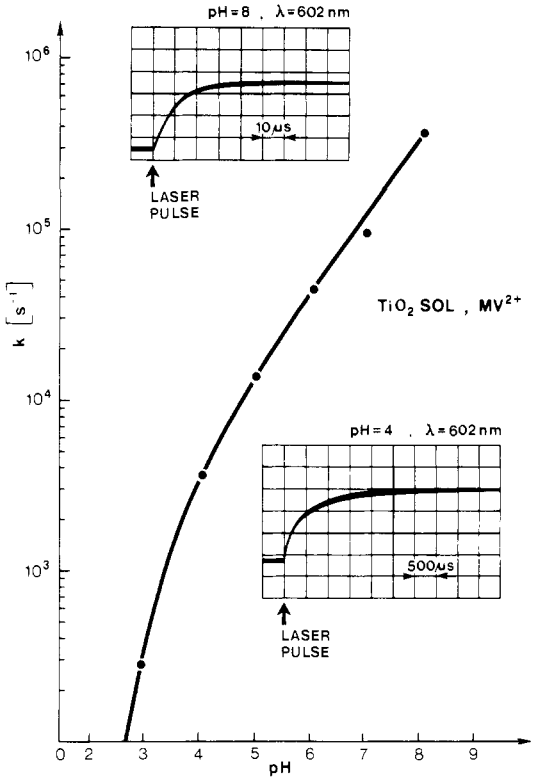

Figure 6. Laser photolysis of TiO_2 colloids (500 mg/L) at various pH values. Effect of pH on the rate constant of electron transfer from the conduction band to MV^{2+}; $[MV^{2+}] = 10^{-3}$ M. Insert: oscilloscope traces illustrating growth of MV^+ absorption at pH 8 and 4.

obtained E_{fb} = 0.06 V (NHE) for rutile electrodes at room temperature and pH 0, while values of −0.038 and −0.05 have been measured for the same material by Wrighton[20] and Bard,[21] respectively. The conduction band of our colloids appears to have a more negative potential, which is crucial for water decomposition systems. This shift presumably arises from the different crystal structures of electrodes and particles. The latter are mainly X-ray amorphous with a small proportion of anatase and have a somewhat larger band gap (100–200 mV) than rutile electrodes. As the valence-band position appears to be rather insensitive to the TiO_2 lattice structure,[22] this increase in E_{gap} should reflect itself in a more negative value for E_{fb}, as is observed experimentally.

The position of the conduction band edge of the colloidal TiO_2 particle influences greatly the rate of the interfacial electron transfer. Figure 6 shows kinetic data obtained from the laser photolysis of solutions containing 500 mg/L TiO_2 and 10^{-3} M MV^{2+} at various pH values. The inserted oscillograms illustrate the temporal behavior of the MV^+ absorption at 602 nm for pH 4 and 8, respectively. In both cases the 602 absorbance grows to a plateau according to a first-order rate law. However, while at pH 4 this process requires several milliseconds to come to completion, only a few microseconds are needed at pH 8. The plot of the first-order rate constant for MV^+ formation against pH reveals that k increases by more than 3 orders of magnitude over a pH region from 3 to 8. Further rate enhancement is observed at higher alkalinity where the half-lifetime for MV^{2+} reduction by e^-_{CB} reaches a lower limit of ca. 100 ns, corresponding to a k value of 7×10^6 s^{-1}. The true bimolecular rate constant for the electron-transfer process is here 7×10^9 M^{-1} s^{-1}, which approaches the diffusion-controlled limit.

These phenomena may be rationalized in terms of the shift of the conduction-band position of the TiO_2 particle with pH affecting

(19) Dutoit, E. C.; Cardon, F.; Gomes, W. P. *Ber. Bunsenges. Phys. Chem.* **1976**, *80*, 475.

(20) Bolts, J. M.; Wrighton, M. S. *J. Phys. Chem.* **1976**, *80*, 2641.
(21) Handely, L. J.; Bard, A. J. *J. Electrochem. Soc.* **1980**, *127*, 338.
(22) Kuczynski, L.; Gesser, H. D.; Turner, C. W.; Speers, E. A. *Nature (London)* **1981**, *291*, 399.

the match of electronic donor levels in the semiconductor (E_{sc}^{occ}) with that of acceptor levels in the electrolyte (D_{el}^{unocc}). The overlap integral of these two density-of-state functions determines the rate constant for the tunneling transition of the electron across the interface.[23]

$$k = v\int_0^\infty (D_{sc}^{occ})(D_{el}^{unocc})\,dE \qquad (6)$$

where v is the tunneling collision frequency. D_{sc}^{occ} is identical with the density of occupied electronic levels in the conduction band of the TiO_2 particle, which peaks sharply at the conduction band edge E_{CB}. Thus,

$$(D_{sc}^{occ})_{max} \simeq -0.12 - 0.059(pH) \qquad (7)$$

and in order to derive the maximum in the density-of-state function of unoccupied levels in the electrolyte, we subtract from the potential of the $MV^{2+/+}$ couple the reorganization energy λ, which is estimated as 0.3 eV:

$$(D_{el}^{unocc})_{max} = E°(MV^{2+/+}) - \lambda \simeq -0.745 \qquad (8)$$

From a comparison of eq 5 and 4, one recognizes that under acid conditions there is poor overlap between occupied states in the semiconductor and unoccupied states in the electrolyte. As a consequence the electron transfer is slow or fails to occur. The overlap improves as one increases the pH, and consequently k increases. The rate of reduction of MV^{2+} should reach a maximum under pH conditions where $(D_{sc}^{occ})_{max} = (D_{el}^{unocc})_{max}$, i.e., around pH 10.5. Indeed, we find that k approaches the diffusion-controlled limit at pH >10, where the interfacial electron transfer becomes no longer rate determining.

Dynamics of Light-Induced Hole Transfer from the Valence Band of Colloidal TiO_2 to Electron Donors in Solution. In the previous section we evoked a band model for colloidal TiO_2 particles and light-induced electron-hole separation to explain the reduction of MV^{2+} under near-UV irradiation. If this picture is correct, it should be possible to study separately oxidation processes of the valence-band hole, produced as a complementary species after band-gap excitation. Suitable electron donors added to the electrolyte should be capable of scavenging the hole. We selected SCN^- ions for this purpose. The redox potential of the couple $SCN·/SCN^-$ ($E°$ = +1.5 V)[24] renders a process of the type

$$h^+(TiO_2) + SCN^- \rightarrow SCN· \qquad (9)$$

thermodynamically feasible. Also, the SCN· radical in the presence of excess SCN^- is very rapidly converted into $(SCN)_2^-$, which can be readily identified by its characteristic spectrum in the visible range.

Results obtained from the laser photolysis of solutions containing 500 mg/L colloidal TiO_2 and 0.1 M SCN^- (pH 3) are depicted in Figure 7. The transient absorption present immediately after the light flash is plotted as a function of the detection wavelength. This curve exhibits a pronounced maximum around 470 nm, which can be unambiguously attributed to the $(SCN)_2^-$ radical.[25]

The pathway of $(SCN)_2^-$ formation is indicated schematically in the upper part of Figure 7. Band-gap excitation by the laser leads to electron-hole pair formation. The latter migrates to the semiconductor interface where hole transfer to SCN^- produces the radical SCN·. In a subsequent reaction, SCN· is complexed by excess SCN^- ions to yield the species $(SCN)_2^-$, which is optically observed. As the rate constant for the complexation[26]

$$SCN· + SCN^- \rightarrow (SCN)_2^- \qquad (10)$$

is 7×10^9 M^{-1} s^{-1}, the lifetime of SCN· is only 2 ns under the experimental conditions employed in Figure 7.

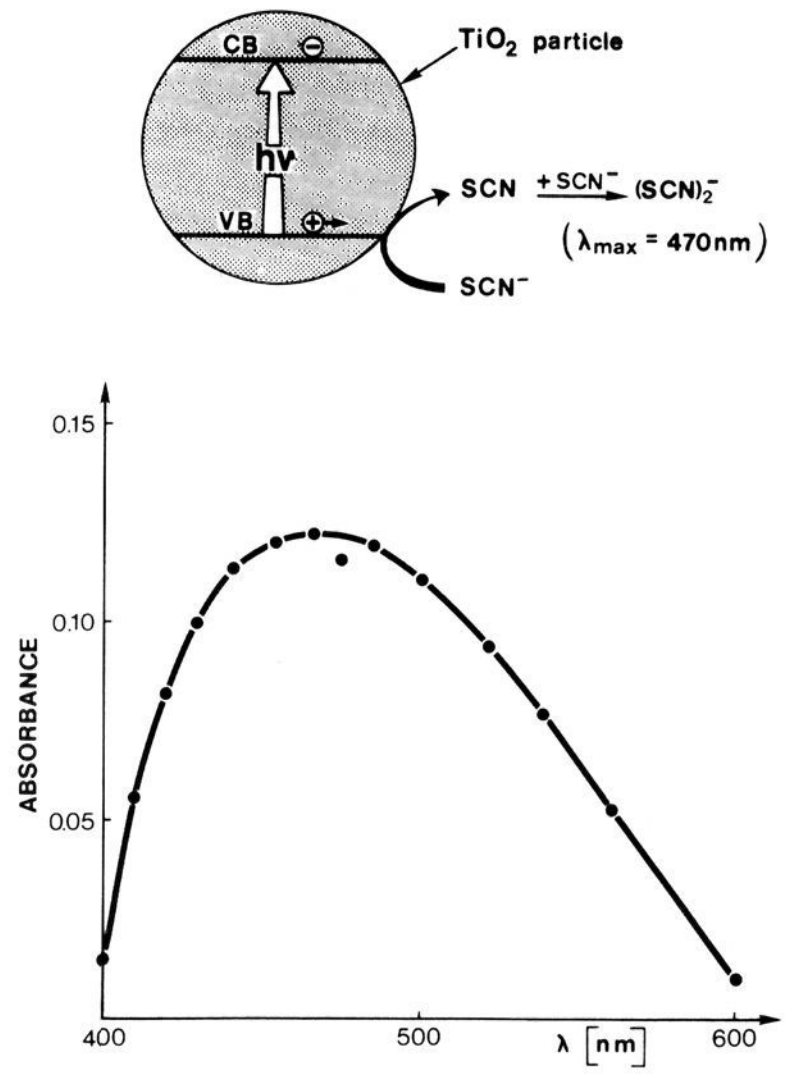

Figure 7. Hole transfer from the valence band of TiO_2 to SCN^-. Transient spectrum obtained at the end of laser pulse from solutions containing 500 mg/L TiO_2 and 0.1 M SCN^- (pH 3).

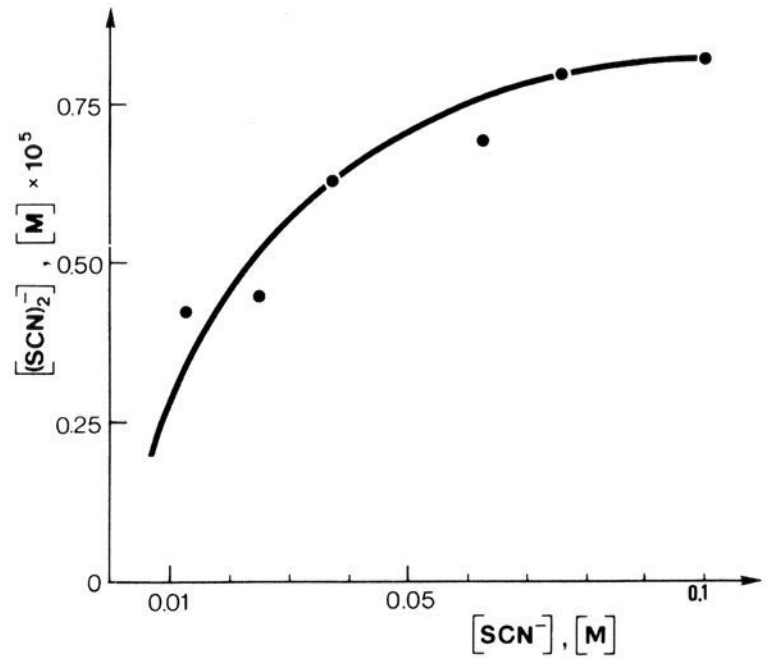

Figure 8. Yield of $(SCN)_2^-$ as a function of SCN^- concentration; conditions as in Figure 5.

The experiments in Figure 7 were conducted in aerated solutions where O_2 might have acted as an acceptor for conduction-band electrons. However, we found that deoxygenation of the solution introduced no significant changes in the yield of $(SCN)_2^-$. Apparently the capture of holes by SCN^- is fast enough for it not to be affected by conduction-band processes.

In Figure 8 is shown the effect of SCN^- concentration on the amount of $(SCN)_2^-$ produced by the laser pulse. Variation of the donor concentration from 10^{-2} to 1.1×10^{-1} M results in an increase in $[(SCN)_2^-]$ that reaches 7.5×10^{-6} M at the upper limit of SCN^- concentration.

The yield of $(SCN)_2^-$ was found to be affected drastically by the pH and this is illustrated in Figure 9. In striking contrast to the efficiency of MV^{2+} reduction by conduction-band electrons, the concentration of $(SCN)_2^-$ measured at the end of the laser

(23) Gerischer, H. *Pure Appl. Chem.* **1980**, *52*, 2649.
(24) Henglein, A., private communication.
(25) Baxendale, J. H.; Bevan, P. L. T.; Stott, D. A. *Trans. Faraday Soc.* **1968**, *64*, 2384.
(26) Schöneshöfer, M.; Henglein, A. *Ber. Bunsenges. Phys. Chem.* **1969**, *73*, 284.

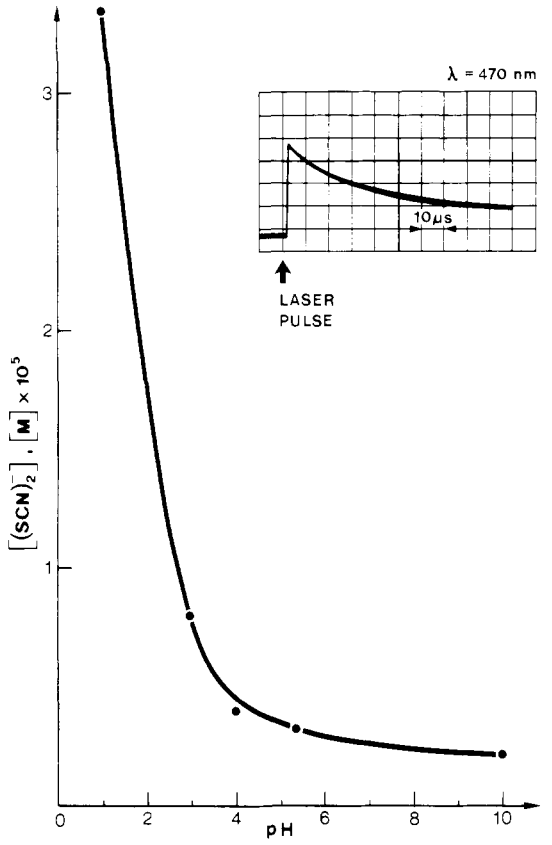

Figure 9. Effect of pH on the yield of $(SCN)_2^-$ measured at the end of the laser flash; $[(SCN)_2^-] = 0.1$ M; $[TiO_2] = 500$ mg/L. Insert: oscilloscope trace showing formation and decay of $(SCN)_2^-$ absorption at 470 nm. pH 3.

flash was found to decrease sharply with increasing pH. Thus at pH 1, $[(SCN)_2^-] = 3.5 \times 10^{-5}$ M, while at pH 3 less than one-fourth of this yield is observed. Further decrease of the $(SCN)_2^-$ yield is observed at higher pH. However, under these conditions, poly(vinyl alcohol) was used to stabilize the TiO_2 particles. Therefore, this effect cannot be attributed unambiguously to the decrease in proton concentration as it might result simply from the competition of the protective agent for valence-band holes.

There is a further important difference to note between MV^{2+} reduction by e^-_{CB} and SCN^- oxidation by h^+ that concerns the kinetics of the charge-transfer process. For all SCN^- concentrations and pH values investigated the $(SCN)_2^-$ signal always appeared promptly with the laser pulse and there was no indication of any further growth. The features of the oscillogram inserted in Figure 9 are typical for the kinetic observations made with this system. The 470-nm absorption of $(SCN)_2^-$ rises concomitantly and within the light pulse and decays thereafter over a time period of 100–200 μs. Kinetic analysis showed that the decay process followed second-order kinetics, the rate constant being 7.5×10^9 M^{-1} s^{-1}.

The prompt nature of the SCN^- oxidation by valence-band holes would suggest that this process involves predominantly SCN^- species adsorbed to the TiO_2 surface. This eliminates the need for diffusion of the reactant to the particle, allowing the hole transfer to proceed at a very high rate. One could also reason that the hole transfer has to be very rapid to compete successfully with oxidation of water to adsorbed OH radicals.

$$h^+ + H_2O \rightarrow (OH)_{ads} + H^+ \qquad (11)$$

Such an interpretation is supported by the pH effect on the $(SCN)_2^-$ yield. We recall that the valence band of TiO_2 shifts cathodically by 59 mV per increasing pH unit. While this does not affect the driving force for water oxidation, it decreases that for hole transfer to SCN^-. Thus in the competition of the two processes, water oxidation is favored upon increasing the pH, reducing the yield of $(SCN)_2^-$.

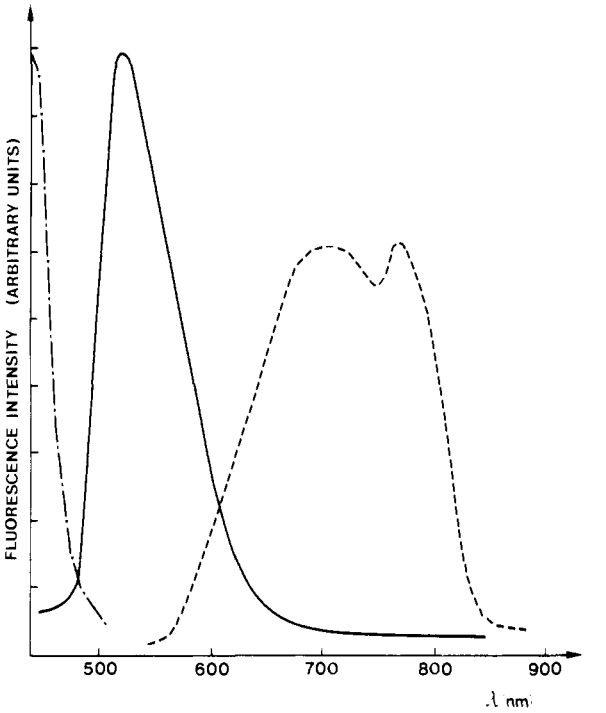

Figure 10. Luminescence ($\lambda_{exc} = 425$ nm) and luminescence excitation ($\lambda_{em} = 640$ nm) spectrum of colloidal CdS ($[CdS] = 3 \times 10^{-3}$ M) in neutral water.

A further important point to consider when discussing pH effects is the charge of the TiO_2 particles, which should influence the adsorption of SCN^-. The point of zero ζ potential of our TiO_2 sol has been determined as 3.3.[4] Below this pH, adsorption is enhanced by Coulombic interaction, leading to an increase in surface concentration of SCN^- and hence high scavenging efficiency.

A final remark in connection with SCN^- oxidation by TiO_2 valence-band holes concerns the fate of the $(SCN)_2^-$ radical. The latter was shown to decay in a diffusion-controlled process following a second-order rate law. Presumably this arises from the dismutation into $(SCN)_2$ and SCN^-.

Transparent Dispersions of CdS, Luminescence, and Luminescence Excitation Spectra. The UV–vis absorption spectrum of the CdS sol has been reported previously.[27] It is distinguished by a sharp band edge rising steeply toward the blue below 520 nm. The onset coincides exactly with the band gap of crystalline CdS electrodes, i.e., 2.4 eV. Excitation of the colloidal particles leads to luminescence with spectral characteristics that are displayed in Figure 10. This emission is distinguished by a broad maximum around 700 nm. Using the single photon counting technique, we determined the decay time of the luminescence as $\tau = 0.3 \pm 0.2$ ns.

The dashed line in Figure 10 represents the excitation spectrum for the luminescence measured at 640 nm. It is identical with the absorption spectrum of the CdS sol. The onset is at 520 nm, the band rising sharply toward the UV. From the perfect coincidence of the excitation with the absorption spectrum, one infers that the luminescence arises truly from band-gap excitation of the CdS particles. The possibility that it originates from excitation of impurities can thus be excluded.

The red shift of the emission with respect to the energy of the band gap is caused by the presence of surface states that can act as radiative recombination sites. This is supported by the effect of methylviologen addition, which produces a blue shift and drastic sharpening of the emission peak, Figure 10. Thus, at 10^{-2} M

(27) Kalyanasundaram, K.; Borgarello, E.; Duonghong, D.; Grätzel, M. *Angew. Chem., Int. Ed. Engl.* **1981**, *20*, 987.

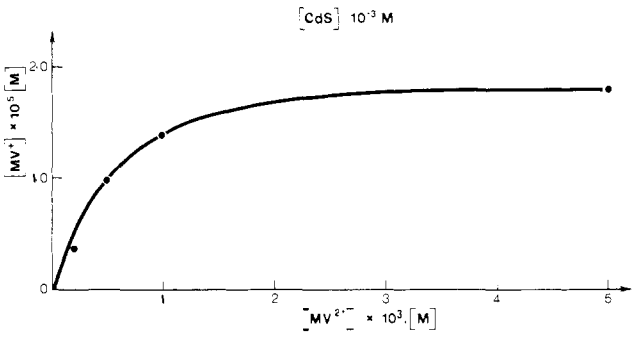

Figure 11. 487-nm laser photolysis of colloidal CdS in the presence of methylviologen. Yield of MV^+ as a function of initial MV^{2+} concentration.

MV^{2+}, the maximum of the luminescence is now located at 524 nm, corresponding almost exactly to the energy difference between valence and conduction band.

The interpretation of this effect is as follows: The drastic influence of MV^{2+} on the emission properties of CdS shows that the former is specifically adsorbed onto the surface of the colloidal semiconductor particles. The interaction with surface states, i.e., dangling bonds, etc., leads to splitting of their energetic position, much in the same way as Ru^{3+} ions split the surface-state levels of GaAs.[28] These states are, therefore, no longer available for radiative recombination, which now takes place exclusively between conduction and valence band.

Electron Transfer from the Conduction Band of Colloidal CdS to Acceptors in Solution. Competitive Trapping of e^-_{CB} by Noble-Metal Deposits. From the short lifetime of an electron-hole pair in colloidal CdS, one would infer that e^-_{CB} could only reduce species adsorbed to the surface of the particle. Diffusional displacement required for reaction with acceptors in the solution bulk would be too slow to be able to compete with $e^-_{CB} \cdots h^+$ annihilation. This idea is fully borne out by experimental results. Thus, in the presence of MV^{2+} as acceptor, the blue color of MV^+ appears promptly and within the laser pulse and no growth of the 602-nm absorption is observed as was the case for TiO_2. In the absence of O_2, the signal of MV^+ remains stable. An intense blue color is developed under continuous exposure to visible light in agreement with the observations made by Harbour and Hair on macrodisperse CdS powders.[29]

Figure 11 reports the yield of MV^+ obtained by flash irradiation of the CdS sol with the 487-nm laser light as a function of the initial MV^{2+} concentration. Increasing the latter from 0.2×10^{-3} to 5×10^{-3} M results in an augmentation of $[MV^+]$ from 0.3×10^{-5} to 2×10^{-5} M. Apparently at the higher MV^{2+} concentration, the coverage of the CdS particle surface with MV^{2+} is increased. This enhances the rate of interfacial electron transfer, which can compete more efficiently with electron-hole recombination. In these experiments there was no hole scavenger present in solution. The complementary valence-band process is therefore

$$CdS + 2h^+ \rightarrow Cd^{2+} + S \qquad (12)$$

In the context of our present investigations of visibl light induced hydrogen generation with CdS dispersions, it appeared to us interesting to examine whether at 5×10^{-3} M MV^{2+} concentration one would still be able to intercept the e^-_{CB} reaction with adsorbed MV^{2+} by a noble-metal catalyst deposited onto the particle surface. The conjecture was that if Pt in ultrafine form was loaded onto CdS, part of the conduction-band electrons would be trapped by Pt sites in competition with MV^{2+} reduction:

$$e^-_{CB} + MV^{2+} \xrightarrow{k(MV^{2+})} MV^+ \qquad (13)$$

$$e^-_{CB} + Pt \xrightarrow{k(Pt)} Pt^- \xrightarrow{+H_2O} {}^1/_2H_2 + OH^- \qquad (14)$$

Electrons undergoing reaction 14 can no longer contribute to the yield of MV^+, as they are used to generate hydrogen from water under the prevailing pH conditions.

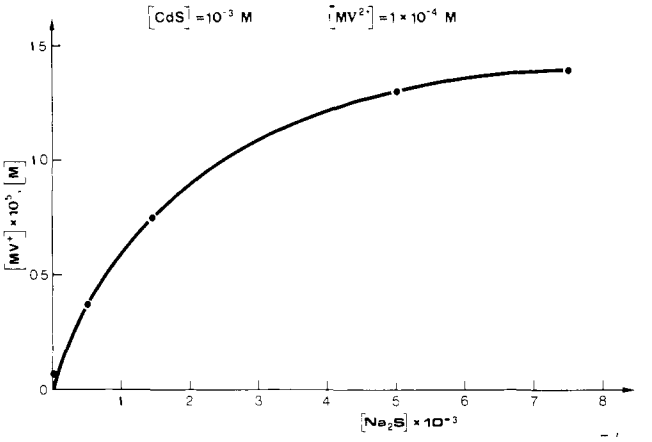

Figure 12. Effect of Na_2S concentration on the yield of MV^+ obtained from the 487-nm laser photolysis of CdS.

This concept was confirmed by the experimental results. The MV^+ concentration produced by the laser pulse in the presence of Pt, $[MV^+]_{Pt}$, was compared to that obtained in Pt-free solution under otherwise identical conditions. The ratio $r = [MV^+]/[MV^+]_{Pt}$ was found to be 1.5 (pH 5). From eq 13 and 14

$$1 - \frac{1}{r} = \frac{k(Pt)[Pt]_s}{k(MV^{2+})[MV^+]_s} = 0.33 \qquad (15)$$

where the subscript indicates surface concentrations. Therefore at 8% Pt loading, one-third of the conduction-band electrons react with Pt[30] despite the high surface coverage by MV^{2+}. This indicates a high-scavenging cross section of the noble-metal deposit for e^-_{CB}. This type of study should lend itself to a detailed investigation of electron-transfer processes from the conduction band of colloidal semiconductors to catalytic sites introduced by metal deposition.

Light-Induced Hole Transfer from the Valence Band of Colloidal CdS to Electron Donors in Solution. This final section will report on some preliminary results concerning the exchange of holes from the CdS valence band to solution species. The first electron donor selected was SH^-, which is known to suppress the photocorrosion of CdS via[31]

$$2h^+ + SH^- \rightarrow S + H^+ \qquad (16)$$

As the course of reaction 16 is difficult to monitor directly by kinetic spectroscopy, we chose an indirect method: A small concentration of MV^{2+} was added to the solution, which in the absence of hole scavenger intervenes very inefficiently in electron-hole recombination. An agent such as SH^-, which removes the hole from the semiconductor, should increase the lifetime of e^-_{CB} and hence the efficiency of MV^{2+} reduction.

Figure 12 shows laser photolysis results obtained with deaerated colloidal CdS solutions (10^{-3} M analytical concentration, pH 7) in the presence of 10^{-4} M MV^{2+}. The concentration of MV^+ present immediately after the laser pulse is plotted as a function of Na_2S concentrations. Only a 2×10^{-7} M MV^+ concentration is produced in the absence of Na_2S. The yield rises steeply upon sulfide addition, reaching a value of 1.5×10^{-5} M at 8×10^{-3} M Na_2S concentration. Apparently the increase in the MV^+ yield arises from the efficient reaction of valence-band holes with SH^- species adsorbed to the surface of CdS. This process must occur at a much faster rate than photocorrosion even at relatively small

(28) Parkinson, B. A.; Heller, A.; Miller, B. *J. Electrochem. Soc.* **1979**, *126*, 454.
(29) Harbour, J. R.; Hair, M. L. *J. Phys. Chem.* **1977**, *81*, 1791.
(30) It may be argued that the reduction of the MV^+ yield in the presence of Pt loading results from a reaction of the former with water to produce H_2 catalyzed by Pt. This process occurs in fact, albeit on a microsecond time scale. The yield of MV^+ measured immediately after the pulse is in the nanosecond time domain and reflects correctly the competition of Pt sites and MV^{2+} for conduction-band electrons.
(31) (a) Ellis, A. B.; Kaiser, S. W.; Wrighton, M. S. *J. Am. Chem. Soc.* **1976**, *98*, 1635. (b) Hodes, G.; Manassen, J.; Cohen, D. *Nature (London)* **1976**, *261*, 403. (c) Miller, B.; Heller, A. *Nature (London)* **1976**, *262*, 680.

concentrations of Na_2S. The scavenging of the hole increases significantly the lifetime of conduction-band electrons resulting in a higher efficiency of interfacial electron transfer to MV^{2+}.

Direct observation of hole transfer from the valence band of a colloidal CdS particle to a solution species is possible when *N*-methyl-2-(carboxymethyl)phenothiazine (MCPTH) is employed as an electron donor.

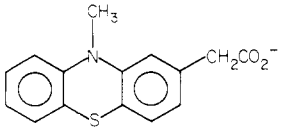

This compound adsorbs strongly to the surface of CdS particles. Its redox potential is 0.69 V (vs. NHE) and the one-electron oxidation product ($MCPTH^+$) has a characteristic absorption with a maximum at 530 nm.[32]

Upon 532-nm laser excitation of colloidal CdS (2×10^{-3} M analytical concentration, pH 6) in the presence of 10^{-3} M MCPTH, one observes formation of a transient whose absorption features are identical with those of the MCPTH cation radical. The appearance of this transient is very fast and follows essentially the time profile of the laser pulse. By use of an extinction coefficient for the cation radical of 9900 M^{-1} cm^{-1}, the concentration of $MCPTH^+$ present after the laser pulse was evaluated as 10^{-7} M.

We were interested in checking whether the yield of $MCPTH^+$ could be increased by depositing a small amount of hole-transfer catalyst, i.e., RuO_2, onto the particle surface.[6,27] The experiment was therefore repeated with CdS particles having a loading of 1% RuO_2.[33] A striking increase in the yield of $MCPTH^+$ was observed that was at least 10 times higher than that obtained in the absence of RuO_2. This experiment provides unambiguous evidence for the acceleration of interfacial hole transfer by the RuO_2 deposit. We have proposed earlier that such a catalytic effect is the basis of light-induced water decomposition observed with CdS dispersions loaded simultaneously with RuO_2 and Pt.[6,27]

(32) These measurements have been performed by Dr. D. Serve, visiting scientist from the University of Grenoble, France, in our laboratory and will be published shortly.

(33) The deposit of RuO_2 was produced by adding a solution of RuO_4 to the CdS dispersion as described in ref 6 and 27.

Conclusion

This is the first direct observation of the dynamics of interfacial electron- and hole-transfer processes from colloidal semiconductors to electron donors and acceptors in solution. A first result emerging from the present study concerns the solid-state characteristics of these particles. Despite their minute size and amorphous character, they exhibit band structure similar to the macroscopic and crystalline material. This manifests itself by distinct absorption and emission features and the fact that selective oxidation or reduction reactions can be performed with valence-band holes and conduction-band electrons, respectively, after light excitation of the particle. Important information on the dynamics of interfacial electron transfer has been obtained, which to a large extent is determined by the match of electronic levels of donor and acceptor states separated by the semiconductor/water interface. From these studies the position of the conduction or valence band of a colloidal semiconductor particle can be obtained that may deviate significantly from the value obtained for macroelectrodes. Work involving a series of different electron donors and acceptors is now in progress. This should yield a wealth of information on the detailed mechanism of charge-transfer processes across the semiconductor/electrolyte interface.

Acknowledgment. This work was sponsored by the Swiss National Science Foundation and CIBA Geigy, Basel, Switzerland. We are grateful to Dr. G. Hodes, Weizmann Institute, Israel, and Drs. N. Bühler and K. Meier, CIBA Geigy, Basel, for critical reading of the manuscript.

Registry No. TiO_2, 13463-67-7; CdS, 1306-23-6; BDH, 4685-14-7.

Microscopic Environment of Poly(styrenesulfonate) Macroanions. Emission and Absorption Spectra, Lifetime, and Depolarization Measurements of a Cationic Fluorescence Probe under High Pressure

Nicholas J. Turro and Tsuneo Okubo*[1]

Contribution from the Department of Chemistry, Columbia University, New York, New York 10027. *Received August 3, 1981*

Abstract: The absorption and fluorescence spectra, lifetimes, and fluorescence depolarizations of a cationic fluorescence probe, (11-(3-hexyl-1-indolyl)undecyl)trimethylammonium bromide, have been measured in the presence of poly(styrenesulfonate) macroanions. The probe is found to be strongly associated with the macroanions in an environment whose apparent microviscosity is ca. 150 cP. It is concluded that the hydrophobicity and viscosity experienced by the probe associated with poly(styrenesulfonate) ions are extremely high compared with those of the probe associated with typical micelles formed from ionic detergents.

Sodium poly(styrenesulfonate) (NaPSS) is a strongly hydrophobic synthetic macroanionic polymer. The chemical structure of this polyelectrolyte is well characterized and is quite simple when compared with polyelectrolytes that compose biomolecules. Knowledge of the physicochemical properties of NaPSS in solution may be helpful for the understanding of the fundamental aspects of solutions of more complex biomolecules. Many thermodynamic and kinetic studies on NaPSS in which hydrophobic interactions were found to be very important in the determination of solution properties have been reported;[2] i.e., electrostatic interactions alone

(1) Department of Polymer Chemistry, Kyoto University, Kyoto, Japan.

0002-7863/82/1504-2985$01.25/0